Low-energy structure of the even-A $^{96-104}$Ru isotopes via g-factor measurements

M. J. Taylor,[1,*] G. Gürdal,[2] G. Kumbartzki,[2] N. Benczer-Koller,[2] A. E. Stuchbery,[3] Y. Y. Sharon,[2] M. A. Bentley,[1] Z. Berant,[4,5] R. J. Casperson,[4] R. F. Casten,[4] A. Heinz,[4,†] G. Ilie,[4] R. Lüttke,[4,6] E. A. McCutchan,[4] J. Qian,[4] B. Shoraka,[7,4] V. Werner,[4] E. Williams,[4] and R. Winkler[4]

[1]*Department of Physics, University of York, York YO10 5DD, UK*
[2]*Department of Physics and Astronomy, Rutgers University, New Brunswick, New Jersey 08903, USA*
[3]*Department of Nuclear Physics, RSPE, Australian National University, Canberra, Australian Capital Territory 0200, Australia*
[4]*Wright Nuclear Structure Laboratory, Yale University, New Haven, Connecticut 06520, USA*
[5]*Nuclear Research Center Negev, Beer-Sheva 84190, Israel*
[6]*Technical University Darmstadt, Darmstadt 64277, Germany*
[7]*Department of Physics, University of Surrey, Guildford GU2 7XH, UK*

(Received 17 February 2011; published 25 April 2011)

The transient-field-perturbed angular correlation technique was used with Coulomb excitation in inverse kinematics to perform a systematic measurement of the g factors of the first excited 2_1^+ states in the stable even-A isotopes $^{96-104}$Ru. The measurements have been made relative to one another under matched kinematic conditions and include a measurement of $g(2_1^+) = +0.47(3)$ in ^{96}Ru.

DOI: 10.1103/PhysRevC.83.044315 PACS number(s): 21.10.Ky, 23.20.En, 25.70.De, 27.60.+j

I. INTRODUCTION

Measurements of the fundamental observables of excited nuclear states, such as magnetic moments, help shed light on the excited states' wave functions. With the aid of theoretical models, such measurements can reveal detailed nuclear structure information. In particular, the systematic measurement of the magnetic moments of a particular excited state (same J^π) across an isotopic chain can yield information on the evolution of nuclear structure as a function of neutron number. Such measurements in the $A \approx 100$ region have highlighted some complex structure changes [1], with nuclei exhibiting both shape coexistence and shape transitions (sudden onsets of deformation) with the addition of only a few nucleons. Magnetic moment measurements of first excited 2_1^+ states in even-even nuclei in this region [1–3] have also provided evidence for the emergence and weakening of an $N = 56$ subshell closure with increasing proton number. The stable even-mass ruthenium isotopes $^{96-104}_{44}$Ru, with protons half-filling the $Z = 38$–50 shell and neutrons filling orbitals above $N = 50$, present an ideal laboratory to study, via magnetic moment measurements of the 2_1^+ states, the transition between single-particle and collective excitations, as well as the evolution of the $N = 56$ subshell closure.

The first measurements of the g factors of the 2_1^+ states in the stable even-A Ru isotopes were those by Auerbach *et al.* [4], who used a perturbed angular correlation (PAC) technique to study the isotopes ^{100}Ru and ^{102}Ru. The excited 2_1^+ states were populated, respectively, by the radioactive decays of ^{100}Rh and ^{102}Rh, which were dissolved in ferromagnetic host lattices. The $g(2_1^+)$ in ^{102}Ru was later remeasured with improved statistical precision by Johansson *et al.* [5], again using the PAC method with ^{102}Rh being dissolved in a ferromagnetic lattice.

Measurements of $g(2_1^+;^{98}\text{Ru})$ and $g(2_1^+;^{104}\text{Ru})$ were reported by Heestand *et al.* [6], who used an ion implantation perturbed angular correlation (IMPAC) technique in which both the transient and static hyperfine fields affected the extracted g factors. These experiments were performed at a time when little work had been done to accurately parametrize the transient-field (TF) strength experienced by ions traversing a ferromagnetic foil. The results from the IMPAC measurements were subsequently reanalyzed on the basis of the Lindhard-Winther [7] model for the transient field by Hubler *et al.* [8]. This model, however, is now known to give an incorrect velocity dependence for the transient field [9,10]. The g factor of the first excited 2_1^+ state in ^{96}Ru had not been measured prior to the present experiment.

The current literature values for $g(2_1^+;^{98,100,102,104}\text{Ru})$ [11–14] [see Fig. 1(a)] are consistent, within their somewhat large associated uncertainties ($\sim$75% for ^{98}Ru), with each other and with the predictions of the hydrodynamical model ($g = Z/A$), suggesting a possible collective nature for the 2_1^+ states. This almost constant trend of the g-factor data is not, however, observed in either the energies of the 2_1^+ states [11–15] [Fig. 1(b)], which show a steady decrease with N, or the B(E2:$0_1^+ \rightarrow 2_1^+$) values [12,15–17] [Fig. 1(c)], which increase with increasing N. The latter two observables suggest increased collectivity with increasing neutron number.

In light of the large uncertainties on the previously measured g factors, and since there are serious questions about the reliability of the IMPAC results, it became imperative to remeasure, with greater accuracy, the g factors of the even-even $^{98-104}$Ru isotopes. Moreover, in order to obtain a better understanding of the evolution of collectivity in the low-energy structure of the stable even-A Ru nuclei, it was considered important to measure $g(2_1^+)$ in the $N = 52$ nucleus ^{96}Ru.

*Present address: School of Physics and Astronomy, Schuster Laboratory, University of Manchester, Manchester M13 9PL, UK; m.j.taylor@manchester.ac.uk
†Present address: Fundamental Physics, Chalmers University of Technology, Gothenberg, SE-412 96 Sweden

 ©2011 American Physical Society

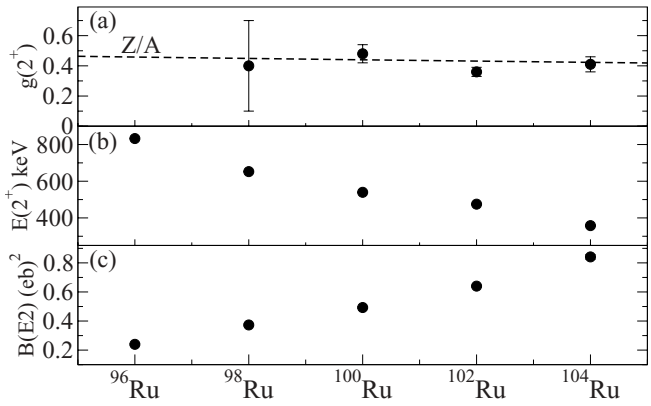

FIG. 1. (a) Current literature values for the $g(2_1^+)$ states for the stable even-A Ru isotopes (circles), along with predictions from the hydrodynamical model (dashed line). (b) Excitation energies of the first excited 2_1^+ states and (c) B(E2:$0_1^+ \rightarrow 2_1^+$) values for $^{96-104}$Ru (uncertainties smaller than symbol size). The data are taken from Refs. [11–17].

II. EXPERIMENTAL TECHNIQUE

The transient-field-perturbed angular correlation technique [18], combined with Coulomb excitation in inverse kinematics [19], was used. Isotopically pure Ru beams were accelerated by the ESTU tandem accelerator of the Wright Nuclear Structure Laboratory at Yale University. The beams were incident upon four different multilayered targets. As summarized in Table I, the first layer of each target consisted of an isotope (^{12}C, ^{24}Mg, or ^{26}Mg) in which the Ru beam nuclei were Coulomb excited to their 2_1^+ state. The excited Ru nuclei then traversed a ferromagnetic Gd layer, which was magnetized by an external field of 0.073 T, perpendicular to the scattering plane, and whose direction was reversed every 2 minutes to minimize systematic errors. While in the Gd layer, the spins of the excited Ru nuclei precessed about the vertical axis due to the interaction of their magnetic moment with the transient hyperfine field. Finally, the excited nuclei were stopped in a hyperfine, interaction-free layer of Cu. Layers of Ni and Ta were used to assist adhesion between the Gd and Cu layers.

The targets were mounted on the tip of a helium Displex refrigerator and were cooled to ∼80 K. The magnetization of each target was measured with the Rutgers AC magnetometer [20] as a function of applied external field and temperature. The target magnetizations, also shown in Table I, were observed to remain constant over a range of temperatures (50–100 K).

TABLE I. Characteristics of the targets used in this work. The target thicknesses are given in mg/cm^2. The magnetization quoted corresponds to an external magnetizing field of 0.073 T and a target temperature of 80 K, conditions similar to those pertaining to this experiment.

Target	^{26}Mg	Gd	Ni	Cu	M(T)
I	0.45	3.2	0.01	5.4	0.205(10)
Target	^{12}C	Gd	Ta	Cu	M(T)
II	0.606	6.426	1.0	11.2	0.178(9)
Target	^{12}C	Gd	Ta	Cu	M(T)
III	0.44	3.34	1.4	4.49	0.186(9)
Target	^{24}Mg	Gd	Ta	Cu	M(T)
IV	0.5	3.4	1.0	5.4	0.185(9)

The emitted $2_1^+ \rightarrow 0_1^+$ de-excitation γ rays were detected by four segmented Clover detectors, situated around the target chamber in the horizontal plane at a distance of 132 mm from the target position. Their faces were shielded by a combination of Cu/Cd/Pb absorbers. For the precession measurements, the detectors were positioned at angles of $\pm 67^\circ$ and $\pm 113^\circ$ with respect to the beam axis. At these angles, the counting rate and the slope of the particle-γ angular correlation were optimized.

Particle-γ correlations were measured by recording the Ru γ rays in coincidence with the recoiling ^{12}C, ^{24}Mg, or ^{26}Mg target nuclei detected in a 100-μm-thick circular Si detector of radius 9.8 mm. The Si detector was located 23 mm downstream of the target, subtending a maximum recoil detection angle of $\pm 23^\circ$ with respect to the beam axis. To prevent radiation damage to the Si detector, its face was covered by a 5.6 mg/cm^2 Cu foil to stop any beam ions that emerged from the target. All of the detector signals were processed by XIA digital electronics modules [21]. Beam energies were maintained somewhat below the Coulomb barrier so as to help minimize excitations to states above the 2_1^+ states.

The spin precession angle, $\Delta\theta$, of the Ru magnetic moments, resulting from the coupling of these moments to the transient hyperfine field, is given by

$$\Delta\theta = -g\frac{\mu_N}{\hbar}\int_{t_{\rm in}}^{t_{\rm out}} B_{\rm TF}[v(t), Z]e^{-t/\tau}\,{\rm d}t, \qquad (1)$$

where g is the nuclear state g factor and $B_{\rm TF}$ is the transient field. The integration is performed over the time the excited nucleus spends in the Gd foil. The exponential term takes into account the nuclear decays that take place while the ion is in flight through that foil. This effect becomes significant if τ, the mean life of the excited state, is of the same order as, or shorter than, the transit time through the ferromagnetic layer. The dependence of the transient field on the ion velocity and atomic number has been studied empirically, and the strength of the field can be obtained from a fit to data on known g factors [18,22]. The TF strength can also be determined from the measurement of a known g factor in a neighboring nucleus (similar Z) performed under similar kinematic conditions (similar $v(t)$).

In terms of experimental data, the precession angle $\Delta\theta$ is defined as $\varepsilon(\theta)/S(\theta)$, where $S(\theta)$ is the logarithmic slope of the angular correlation and $\varepsilon(\theta)$ is the ratio of the transition counting rates corresponding to each field direction observed in each Clover detector [23]. In this work, both $S(\theta)$ and $\varepsilon(\theta)$ were directly determined using a split Clover analysis technique, as described in Refs. [24,25]. Because all of the Clover detectors lie in the horizontal plane, vertically aligned segments reside at the same angle with regard to the target position. Hence, analyzing the data separately for each Clover half (thus creating two sets of four detectors) increases the resolution by reducing the Doppler broadening of the γ rays due to the smaller detector opening angles. Angular correlation data (for the $2_1^+ \rightarrow 0_1^+$ transition) obtained from each Clover segment at positions of 50°, 67°, and 80° in each quadrant,

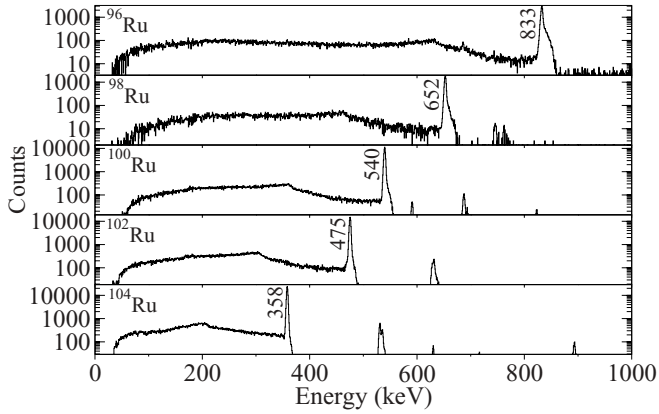

FIG. 2. ^{26}Mg coincident γ-ray spectra, as recorded by a single Clover detector, for all of the Ru isotopes studied. Random coincidences have been subtracted, and a Compton add-back analysis was performed. All spectra are shown on a log scale, and the $2_1^+ \rightarrow 0_1^+$ peak for each isotope is labeled with the transition energy.

were fitted with different separation angles. The best χ^2 fit was obtained for a separation angle of the clover halves of 15.4°, corresponding to effective detector positions of $\theta_{\rm det} = \theta_{\rm Clover} \pm 7.7°$. The relative efficiency for each Clover segment was determined from data taken with a ^{152}Eu source placed at the target position. The $\Delta\theta$, as measured by each Clover half (at 59.3° and 74.7°), was then derived separately. These independent data were in excellent agreement with each other, demonstrating the quality of the data and the effectiveness of the split Clover technique.

Measurements of neighboring $g(2_1^+;^{106}{\rm Pd})$ were also performed using Targets I, II, and III to serve as calibration points for the TF. The measurements were performed under kinematic conditions that replicated those for the Ru isotopes. Higher-lying-state g factors were also measured and reported in Ref. [26].

III. RESULTS

Fig. 2 shows γ-ray spectra in coincidence with recoiling ^{26}Mg target nuclei, as recorded for each of the Ru isotopes studied, using Target I, by one of the Clover detectors at 67°. A Compton add-back analysis was performed for each Clover segment, and random coincidences were subtracted. The spectra shown in Fig. 2 are very clean; the γ rays de-exciting the 2_1^+ states are well resolved and clearly dominate the spectra. The observed $2_1^+ \rightarrow 0_1^+$ transitions for ^{96}Ru and ^{98}Ru (833 and 652 keV, respectively) show clearly extended line shapes due to the short mean lifetimes of the states, 4.05 and 7.93 ps, respectively. Due to the logarithmic scale, peaks pertaining to transitions from higher-lying states can also be seen. Although these transitions feed into the 2_1^+ state, their intensity is negligible.

Table II summarizes the calculated velocities and transit times for the targets and isotopes studied in this work, along with the measured precession angles. As can be seen from the table, the relative $g(2_1^+)$ factors of each of the even-A Ru isotopes were measured under very similar kinematic conditions, using either Target I or Target II. This approach determines the relative g factors independent of a precise knowledge of $B_{\rm TF}$; however, an accurate evaluation of the field strength is important when considering the absolute g factors.

The absolute scale of the experimental g factors has been determined by reference to previous measurements on ^{106}Pd using the external-field and radioactivity techniques [5,27]. Combining the present measurements on Targets II and III with measurements performed at the Australian National University (ANU)[1] [28] a ratio of $g(2_1^+;^{102}{\rm Ru})/g(2_1^+;^{106}{\rm Pd}) = 1.09(2)$ was obtained. Adopting $g(2_1^+;^{106}{\rm Pd}) = +0.39(2)$,[2] $g(2_1^+;^{102}{\rm Ru}) = +0.43(3)$, where the uncertainty is dominated by the uncertainty on the g factor in ^{106}Pd. This value for $g(2_1^+;^{102}{\rm Ru})$ was then used in the evaluation of the absolute g factors for the other measured isotopes.

From the measured precession angles, $\Delta\theta$, and the effective time period over which the transient field was acting, $T_{\rm TF}$ (Table II), an effective TF strength,

$$B_{\rm TF} = \frac{\Delta\theta}{(\mu_N/\hbar) g T_{\rm TF}}, \qquad (2)$$

can be derived. The experimental values of $B_{\rm TF}$ are shown in Fig. 3 for the ^{102}Ru precession angles measured with the four targets detailed in Table I. Because the targets have different magnetizations, and therefore different $B_{\rm TF}$ scales, the field strengths were normalized to the Gd saturation magnetization value of 0.2116 T. The solid line in Fig. 3 represents the effective TF, as a function of ion velocity, using the Rutgers parametrization [10] and a g factor of +0.53. This g factor is larger than that obtained by the analysis based on the ^{106}Pd g factor from IPAC measurements (dashed line in Fig. 3). At the present time, it is not clear why this discrepancy occurs. Given the potential metallurgical issues with target preparation in IPAC measurements, as well as the lack of an independent measurement to calibrate the TF in this region, future measurements will be required in order to clarify the situation.

IV. DISCUSSION

The experimental g factors relative to $g(2_1^+;^{106}{\rm Pd})$ are shown in Table III. Figure 4 compares the measured $g(2_1^+)$ factors from this work with values from the current literature and the predictions of the hydrodynamical model ($g = Z/A$). The present measurements have smaller uncertainties but agree, within error, with the literature values, although the

[1]For Target I, $g(2_1^+;^{102}{\rm Ru})/g(2_1^+;^{106}{\rm Pd}) = 1.09(6)$. Combining this result with two independent measurements on two other targets at ANU resulted in $g(2_1^+;^{102}{\rm Ru})/g(2_1^+;^{106}{\rm Pd}) = 1.12(3)$, in agreement with the average of the ratios obtained from Targets II and III—namely, $g(2_1^+;^{102}{\rm Ru})/g(2_1^+;^{106}{\rm Pd}) = 1.06(3)$.

[2]The adopted ^{106}Pd g factor is the the weighted average of a measurement by Johansson *et al.* using a Co host [5] and an earlier external-field measurement with which it agrees [27]. After making a small correction for a more recent level lifetime ($\tau = 17.6(9)$ ps [29]), a $g(2_1^+;^{106}{\rm Pd}) = +0.39(2)$ was obtained, with the uncertainty dominated by the uncertainty in the lifetime.

TABLE II. Kinematics for the Ru isotopes studied for the four targets used. $\langle v_{in}/v_0\rangle$ and $\langle v_{out}/v_0\rangle$ are the mean velocities, relative to the Bohr velocity v_0, for Ru ions on entrance to and exit from the Gd layer, respectively. $\langle v/v_0\rangle$ is the mean velocity of the Ru nuclei, and T_{TF} is the effective time period over which the transient field is acting. Measured precession angles ($\Delta\theta$) and values of evaluated $g(2_1^+)$, calibrated relative to an independent measurement of $g(2_1^+;^{106}\text{Pd}) = +0.39$, are also detailed.

Nucleus	E_{Beam} (MeV)	$\langle v_{in}/v_0\rangle$	$\langle v_{out}/v_0\rangle$	$\langle v/v_0\rangle$	T_{TF} (ps)	$\Delta\theta$ (mrad)	$g(2_1^+)$[a]
Target I							
^{96}Ru	230	5.59	3.40	4.42	0.40	-30.70 ± 1.50	$+0.52 \pm 0.02$
^{98}Ru	230	5.59	3.45	4.44	0.41	-28.90 ± 1.90	$+0.48 \pm 0.03$
^{100}Ru	227	5.55	3.45	4.41	0.42	-27.73 ± 0.94	$+0.45 \pm 0.02$
^{102}Ru	227	5.55	3.49	4.43	0.42	-26.50 ± 0.90	$+0.43 \pm 0.02$
^{104}Ru	227	5.54	3.52	4.45	0.42	-24.82 ± 0.87	$+0.40 \pm 0.01$
^{102}Ru[b]	240	5.81	3.74	4.69	0.40	-31.20 ± 0.97	
^{106}Pd[b]	240	5.78	3.73	4.67	0.40	-30.03 ± 1.48	
Target II							
^{96}Ru	280	7.88	3.56	5.51	0.62	-37.38 ± 1.40	$+0.44 \pm 0.02$
^{98}Ru	280	7.86	3.63	5.51	0.65	-41.05 ± 1.76	$+0.47 \pm 0.02$
^{100}Ru	280	7.81	3.67	5.51	0.66	-38.37 ± 1.06	$+0.43 \pm 0.01$
^{102}Ru	280	7.77	3.71	5.50	0.67	-38.81 ± 0.83	$+0.43 \pm 0.01$
^{104}Ru	280	7.73	3.74	5.51	0.67	-35.79 ± 0.95	$+0.39 \pm 0.01$
^{106}Pd	280					-39.69 ± 1.04	
Target III							
^{102}Ru	160	5.75	3.61	4.58	0.42	-25.02 ± 2.29	
^{102}Ru	227	7.11	4.98	5.98	0.32	-19.87 ± 1.08	
^{106}Pd	230	7.03	4.92	5.91	0.32	-17.73 ± 0.77	
Target IV							
^{102}Ru	227	5.69	3.50	4.50	0.44	-25.06 ± 0.86	

[a]Uncertainties correspond to the statistical uncertainty in the precession measurement only.
[b]Work done at ANU; see Ref. [28].

$g(2_1^+;^{102}\text{Ru})$ value is 20% larger than $g = +0.36(3)$ from Ref. [5]. This value should be re-evaluated or remeasured; indeed, Johansson *et al.* have already questioned (Ref. [5]) the integrity of the metallurgical procedure used in the preparation of the rhodium-iron alloys.

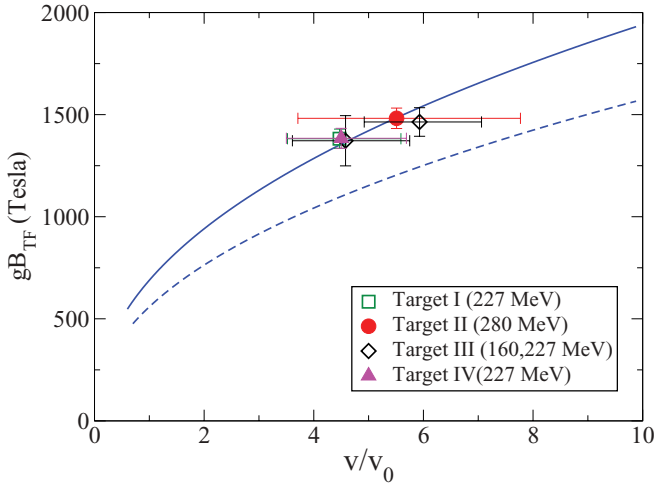

FIG. 3. (Color online) Effective transient-field strengths for the ^{102}Ru precession-angle measurements performed in this work. The experimental values of B_{TF} were calculated using Eq. (2) with $g = 1$. The solid and dashed lines represent the Rutgers parametrization for $g = +0.53$ and $+0.43$, respectively.

The trend in Fig. 4, with $g(2_1^+)$ consistently close to Z/A for $^{96-104}$Ru ($N = 52$–60), is in contrast to the trend observed in the neighboring $^{94-102}$Mo isotopes (see Fig. 5). There, a transition from single-particle to collective structures is exhibited with increasing N [1]. The difference is especially marked between the two $N = 52$ isotones: $g(2_1^+;^{94}\text{Mo}) = +0.31(4)$ and $g(2_1^+;^{96}\text{Ru}) = +0.47(3)$. In ^{94}Mo, the $g(2_1^+)$ is

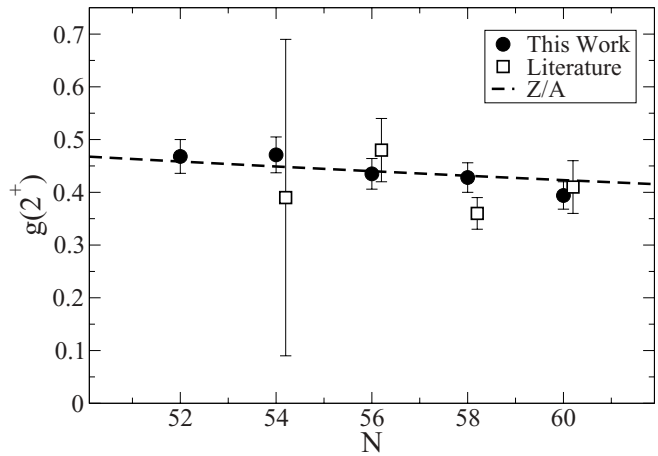

FIG. 4. Measured $g(2_1^+)$ factors from this work for the isotopes $^{96-104}$Ru (circles), along with the prediction of the hydrodynamical model ($g = Z/A$) (dashed line) and values from the current literature (squares).

TABLE III. Energies, mean lifetimes, currently adopted literature values, and g factors obtained in this work for the 2_1^+ states in the even-A $^{96-104}$Ru and ^{106}Pd isotopes.

Isotope	$E(2_1^+)$ (keV)	τ (ps)	$g(2_1^+)$	
			Refs. [2,5,10–14]	This work[a]
^{96}Ru	833	4.24(9)		+0.47(1)(3)
^{98}Ru	652	7.93(115)	+0.39(30)	+0.47(2)(3)
^{100}Ru	540	18.12(19)	+0.48(6)	+0.44(1)(3)
^{102}Ru	475	26.40(29)	+0.36(3)	+0.43(1)(3)
^{104}Ru	358	81.37(144)	+0.41(5)	+0.39(1)(3)
^{106}Pd	512	17.6(9)	+0.40(3)	[+0.39(2)][b]

[a]The first parentheses, the error value, indicate the statistical uncertainty in the relative g-factor values. The second parentheses include the uncertainty in the absolute value, dominated by the uncertainty on the calibration value.
[b]Calibration value.

30% below Z/A, which was attributed to the weak coupling between valence proton and neutron excitations [1]. The level energy spectrum for ^{94}Mo exhibits many single-particle features, and shell-model calculations revealed a dominant $\nu(d_{5/2})^2$ configuration. The measured $g(2_1^+)$ for ^{94}Mo is, however, closer to Z/A than predicted by the limited-basis shell model [1]. The more rapid approach to collectivity, as indicated by the 2_1^+ state g factors in Ru as compared to neighboring Mo, can be ascribed to having two more valence protons, resulting in greater collectivity. Interestingly, Figs. 1(b) and 1(c) show, for the Ru isotopes, a more gradual approach to collectivity than is observed in the g factors (with increasing N) for the $E(2_1^+)$ excitation energies and the B(E2;$0_1^+ \rightarrow 2_1^+$) values.

It is difficult to carry out extensive large-scale shell-model calculations for the heavier Ru isotopes, due to the very large model spaces that would be involved. Halse [30] carried out calculations for ^{96}Ru that utilized a $^{88}_{38}$Sr$_{50}$ core and a valence space consisting of $(2p_{1/2}, 1g_{9/2})$ for protons and $(2d_{5/2}, 3s_{1/2}, 2d_{1/2}, 1g_{7/2})$ for neutrons. Halse calculated excited state quadrupole moments and g factors for the 2_1^+, 4_1^+, and 6_1^+ states. The calculated $g(2_1^+) = +0.66$ is not in agreement with the newly measured $g(2_1^+;^{96}\text{Ru}) = +0.47(3)$. The deviation from $Z/A = 0.45$ for the $g(2_1^+;^{94}\text{Mo}) = +0.31(4)$ (see Ref. [1] and Fig. 5) shows that the weak-coupling scenario is an appropriate approximation for ^{94}Mo, where neutron excitations seem to be dominant over proton excitations (which have a contribution from the repulsive Coulomb interaction). However, this scenario does not seem to apply to ^{96}Ru. Holt *et al.* [31] carried out, for the even-even $N = 52$ nuclei in this region, a systematic shell-model study of magnetic moments and other properties of the basic low-energy one-quadrupole phonon states. These authors used a low-momentum NN interaction and the same model space as Halse, with the addition of the $h_{11/2}$ neutron orbital. Their analysis indicated the existence of a collective proton-neutron symmetric and mixed-symmetry structure for ^{96}Ru, and they calculated $g(2_1^+) = +0.42$, which is in good agreement with the newly measured value. They did not, however, carry out calculations for the heavier Ru isotopes.

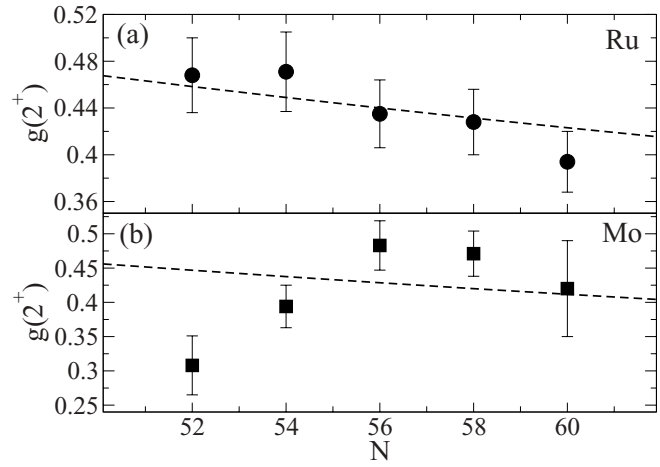

FIG. 5. Comparison between (a) the measured g factors for the Ru isotopes studied in this work, along with Z/A values (dashed line), and (b) the measured g factors for the neighboring Mo isotopes from Ref. [1] and the corresponding Z/A values (dashed line).

The $g(2_1^+)$ values in the heavier even-N Ru isotopes have been calculated within the framework of the neutron-proton interacting boson model (IBM-2) [32] by Sambataro and Dieperink [33]. The results of these calculations, which permit deviations from the Z/A value, generally agree well with the current literature values (within their larger uncertainties) but showed a significant deviation from Z/A for ^{98}Ru. The calculated IBM-2 g factors are shown in Fig. 6 and are compared there to the newly measured values from this work. The comparison shows that the calculated g factors are also in generally good agreement with the more accurate, newly determined g factors for ^{100,102,104}Ru, but deviate somewhat for ^{98}Ru. Unfortunately, the calculation was not extended to ^{96}Ru, and one would not expect this collective approach to work well as closed shells are approached, but if the downward trend shown in Fig. 6 with decreasing N (after $N = 56$) were to continue, the measured $g(2_1^+;^{96}\text{Ru})$ value would not be in agreement with the model. However, with decreasing

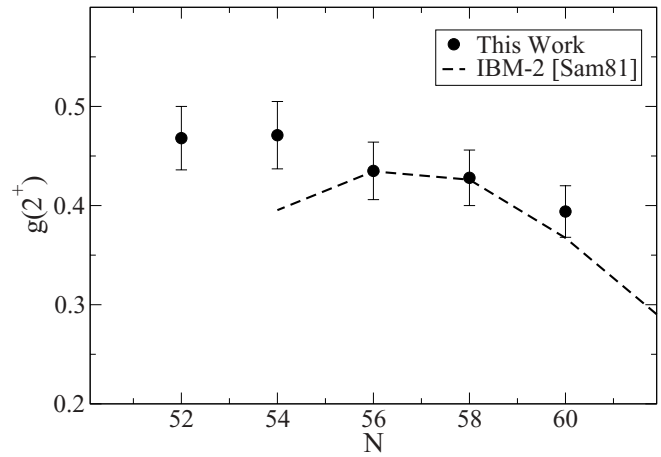

FIG. 6. The measured g factors from this work, along with the results from IBM-2 calculations (Sam81: [33]).

N, one would expect a decrease in the relative influence of the negatively contributing $\nu d_{5/2}$ orbital [$g(\nu d_{5/2})_{\text{Schmidt}} = -0.765$], and therefore an increase in the calculated g factor relative to $g(2_1^+;^{98}\text{Ru})$. Sambataro and Dieperink attributed the large calculated g factor at $N = 56$ to the decreasing influence of the *filled* $\nu d_{5/2}$ orbital on the 2_1^+ state g factor.

Two-neutron separation energy data suggest the existence of an $N = 56$ subshell gap for the Zr isotopes that is reduced somewhat for Mo and disappears for Ru [34,35]. There is evidence of an $N = 56$ subshell closure in the measured g factors of the Zr and Mo isotopes [1,2] that manifests itself as a peak in the g factors at $N = 56$. There is no clear indication from Fig. 4 for such a closure in the Ru isotopes, in agreement with the two-neutron separation energy data.

V. CONCLUSIONS

The g factors for the 2_1^+ states in the stable even-A $^{96-104}$Ru isotopes have been measured relative to one another, using the same target and similar kinematic conditions. This work included the first measurement of $g(2_1^+;^{96}\text{Ru})$ and a remeasurement of $g(2_1^+;^{98-104}\text{Ru})$ with increased accuracy. The absolute g factors were determined from an independently measured $g(2_1^+)$ in ^{106}Pd. All of the measured values are in agreement with the predictions of the hydrodynamical model, indicating a possible collective nature for the 2_1^+ state wave functions. The experimental g factors for $^{100-104}$Ru, remeasured with improved accuracy, are in good agreement with the predictions of the neutron-proton interacting boson model. The data do not show any indication for an $N = 56$ subshell closure, in contrast to the g factors for neighboring Mo and Zr isotopes.

ACKNOWLEDGMENTS

The authors acknowledge and thank the staff of the WNSL for their assistance during the numerous measurements performed there. Thanks to Paul Morrall and P. Maier-Komor for producing the reaction targets. Thanks also to K. O'Grady and N. Aley for measurements and discussions on the magnetic properties of Target I. M.J.T. acknowledges financial support for this work from the Science and Technology Facilities Council. Y.Y.S. acknowledges a sabbatical grant from the Richard Stockton College of New Jersey. This work was supported in part by Australian Research Council Discovery Scheme Grant No. DP0773273, the US National Science Foundation, and the US Department of Energy under Grant No. DE-FG02-91ER-40609.

[1] P. F. Mantica, A. E. Stuchbery, D. E. Groh, J. I. Prisciandaro, and M. P. Robinson, Phys. Rev. C **63**, 034312 (2001).
[2] P. Raghavan, At. Data Nucl. Data Tables **42**, 189 (1989).
[3] G. Jakob, N. Benczer-Koller, J. Holden, G. Kumbartzki, T. Mertzimekis, K.-H. Speidel, C. Beausang, and R. Krücken, Phys. Lett. B **468**, 13 (1999).
[4] K. Auerbach, K. Siepe, J. Wittkemper, and H. J. Körner, Phys. Lett. **23**, 367 (1966).
[5] K. Johansson, E. Karlsson, L.-O. Norlin, R. Å. Windahl, and M. R. Ahmed, Nucl. Phys. A **188**, 600 (1972).
[6] G. M. Heestand, R. R. Borchers, B. Herskind, L. Grodzins, R. Kalish, and D. E. Murnick, Nucl. Phys. A **133**, 310 (1969).
[7] J. Lindhard and A. Winther, Nucl. Phys. A **166**, 413 (1971).
[8] G. K. Hubler, H. W. Kugel, and D. E. Murnick, Phys. Rev. C **9**, 1954 (1974).
[9] J. L. Eberhardt, R. E. Horstman, P. C. Zalm, H. A. Doubt, and G. Van Middelkoop, Hyperfine Interact. **3**, 195 (1977).
[10] N. K. B. Shu, D. Melnik, J. M. Brennan, W. Semmler, and N. Benczer-Koller, Phys. Rev. C **21**, 1828 (1980).
[11] B. Singh and Z. Hu, Nucl. Data Sheets **98**, 335 (2003).
[12] B. Singh, Nucl. Data Sheets **109**, 297 (2008).
[13] D. De Frenne and E. Jacobs, Nucl. Data Sheets **83**, 535 (1998).
[14] J. Blachot, Nucl. Data Sheets **108**, 2035 (2007).
[15] D. Abriola and A. A. Sonzogni, Nucl. Data Sheets **109**, 2501 (2008).
[16] S. Landsberger, R. Lecomte, P. Paradis, and S. Monaro, Phys. Rev. C **21**, 588 (1980).
[17] S. Raman, C. H. Malarkey, W. T. Milner, C. W. Nestor Jr., and P. H. Stelson, At. Data Nucl. Data Tables **36**, 1 (1987).
[18] N. Benczer-Koller, M. Hass, and J. Sak, Annu. Rev. Nucl. Part. Sci. **30**, 53 (1980).
[19] K.-H. Speidel *et al.*, Phys. Rev. C **57**, 2181 (1998).
[20] A. Piqué, J. M. Brennan, R. Darling, R. Tanczyn, D. Ballon, and N. Benczer-Koller, Nucl. Instrum. Methods Phys. Res. A **279**, 579 (1989).
[21] Obtained from X-Ray Instrumentation Associates [www.xia.com].
[22] N. Benczer-Koller and G. J. Kumbartzki, J. Phys. G: Nucl. Part. Phys. **34**, R321 (2007).
[23] M. J. Taylor *et al.*, Phys. Lett. B **605**, 265 (2005).
[24] P. Boutachkov *et al.*, Phys. Rev. C **76**, 054311 (2007).
[25] D. Mücher *et al.*, Phys. Rev. C **79**, 054310 (2009).
[26] G. Gürdal *et al.*, Phys. Rev. C **82**, 064301 (2010).
[27] K. Johansson, L.-O. Norlin, and G. Carlsson, Ark. Fys. **37**, 445 (1968).
[28] S. K. Chamoli *et al.*, Phys. Rev. C (to be published).
[29] S. Raman, C. W. Nestor Jr., and P. Tikkanen, At. Data Nucl. Data Tables **78**, 1 (2001).
[30] P. Halse, J. Phys. G **19**, 1859 (1993).
[31] J. D. Holt, N. Pietralla, J. W. Holt, T. T. S. Kuo, and G. Rainovski, Phys. Rev. C **76**, 034325 (2007).
[32] A. Arima, T. Otsuka, F. Iachello, and I. Talmi, Phys. Lett. B **66**, 205 (1977).
[33] M. Sambataro and A. E. L. Dieperink, Phys. Lett. B **107**, 249 (1981).
[34] S. Anghel, G. Cata-Danil, and N. V. Zamfir, Rom. J. Phys. **54**, 301 (2009).
[35] R. B. Cakirli, R. F. Casten, and K. Blaum, Phys. Rev. C **82**, 061306 (2010).